Title
Evaluation of needle displacement errors in ultraosund-based brachytherapy using electromagnetic (EM) tracking

Author
Samboju, Vishal

Publication Date
2016

Peer reviewed|Thesis/dissertation

Evaluation of needle displacement errors in ultrasound-based brachytherapy using electromagnetic (EM) tracking

by

Vishal Samboju

THESIS

Submitted in partial satisfaction of the requirements for the degree of

MASTER OF SCIENCE

in

Biomedical Imaging

in the

GRADUATE DIVISION

of the

UNIVERSITY OF CALIFORNIA, SAN FRANCISCO

[redacted]

This project would not have been possible without the continued efforts and advisement of the following people: I would like to acknowledge Dr. Chris Diederich's role in the support and completion of this work, all experiments and measurements were conducted through his laboratory. I express deep gratitude for Matthew Adams, who has been an extraordinary mentor and friend, as well as my thesis advisors Dr. Alastair Martin and Dr. Viola Rieke for their time and energy. I would like to thank Dr. Adam Cunha, the committee chair, for allowing me to undertake this process to learn, grow, and discover techniques involved in brachytherapy. Peter Jones and Dr. Vasant Salgaonkar, members of the Diederich lab, also provided critical and valued input during the course of my study.

Evaluation of needle displacement errors in ultrasound-based brachytherapy using electromagnetic (EM) tracking

Abstract:

Purpose

By measuring the discrepancy of distance in electromagnetic tracking (EM) versus ultrasound images to calculate an error due to speed of sound (SOS) variances, this work establishes correctional values for inputs into post processing algorithms that will provide a correction based on B-Mode ultrasound images and consequently radiation dose plans in brachytherapy procedures.

Background

The speed of sound (SOS) within the soft tissue category is approximated to be 1540 m/s [1]. This fixed value is used for the SOS despite actual ranges in vivo varying considerably with one study measuring values of 1450 to 1613m/s in the field of view (FOV) [2]. Brachytherapy for prostate cancer utilizes a transrectal ultrasound (TRUS) probe , which can provide 300-500 micron spatial resolution images for anatomical reference during needle implantation; however, the local composition and configuration of this soft tissue anatomy may exhibit a range of SOSs within the imaging field [3]. Images acquired with a SOS based on 1540 m/s and used in conjunction with stereotactic external coordinate systems can cause image distortion and displacement errors of several millimeters. In combination with the steep $1/r^2$ dose falloff around radioactive seeds, this can lead to erroneous dose delivery [4, 5]. Previous

studies have outlined accuracy of 3-6 mm, leaving ample space for future robotics to overtake the manual process of seed implantation [6].

Method & Materials

The Aurora EM tracking system (NDI Waterloo, Ontario, Canada) generates a 500mm x 500mm x 500mm local electromagnetic (EM) field which can detect the spatial location and orientation of sensors placed within. Philips (Amsterdam, The Netherlands) has developed a brachytherapy needle with an embedded sensor that produces a signal in the EM coordinate system.

Results

Using custom-built phantoms with SOS ranging between 1430 and 1530 m/s, EM tracking resolution was verified to <1 mm precision while US localization resulted in up to 3 mm displacements from physical measurement. We present a model of correction to mitigate error in needle trajectories due to SOS variances and using these values a correctional system will be demonstrated to show the effects of changes in dosimetry due to patient specific SOS variances in the prostate. Results show SOS measurements to be within 1% of measured using a water tank system.

Conclusion

Previous studies have demonstrated that correct speed through tissue can be corrected, but may involve ionizing radiation or physical reference for these corrections [2,7]. The technique proposed will provide a new input of data, derived from the EM modality to approximate a more accurate SOS and result in an evaluation of accuracy of current clinically used systems.

Table of Contents

List of Figures

Page

List of Tables

Page

Introduction:

Brachytherapy Procedures

Prostate cancer is the third most common type of cancer and the most prevalent of cancers in men [8]. Common treatments include radiotherapy, chemotherapy, and surgery. Within the context of radiotherapy procedures, brachytherapy involves the use of radioactive seeds, which are implanted at the site of the tumor. This provides benefits beyond external beam radiation therapy, as it does not require a beam to travel through various layers of tissue to reach the target. In this way brachytherapy seeds can be accurately localized at the site or otherwise optimal proximity to the tumor. This benefit allows more dose to be applied to the cancerous regions, while sparing organs at risk from radiation. However, proper therapy requires conformal and optimized dosimetry plans, which model the patient specifically.

During these procedures, radioactive seeds provide localized dose effectively reducing tumor dimensions and cellularity. For the proper positioning of seeds, a template grid with equally sized boreholes and uniform spacing is utilized to correspond to the planned treatment regions. This template allows for guidance of the catheters and needles through the perineum and to the prostate, providing a coordinate array for corresponding placement. Treatment planning software can be used to recognize these coordinates to place seeds and model dose contours. The template grid is electronically registered onto the US field of view (FOV) based on the speed of sound (SOS) of soft tissue. Thus a discrepancy in distance occurs when the prostate image formed is not truly 1540 m/s in acoustic velocity. In cases which similar size prostates are compared, one with a higher SOS than 1540 m/s and one based on 1540 m/s; the prostate with the higher SOS may appear more compressed than a prostate with an SOS of 1540 m/s.

Imaging in Radiotherapy

In order to localize the needle within the prostate, the development of transrectal ultrasound (TRUS) guidance is used for high temporal resolution of needle position. Previously brachytherapy relied on tactile sensation and palpitation of the prostate by a physician to place sources. The efficacy of brachytherapy greatly improved when ultrasound was introduced into this field and heralded the age of advanced image based treatment planning. Ultrasound imaging provides real time image formation, giving a representation of the anatomy, which the seeds are being placed into.

However, toxicity due to improper seed placement still occurs in cases where implantation outside the prostate results in seed migration, implantation close to the rectum leads to fistulas, implantations in the bladder leads to chronic urinary burning, and implantations too close to the urethra leads to urinary morbidity. Furthermore erroneous dose may contribute to the disease being under or over treated, requiring further hospitalization or treatment [9].

EM Tracking

Consequently needle and catheter localization via imaging becomes an important determinant when defining planned treatment zones for dose distributions. The precision of the dose delivery is vital when organs at risk are in close proximity to the sources. Rather than relying on one imaging modality, many interventional radiology clinics now employ the use of electromagnetic (EM) tracking [8]. These instruments generate localized magnetic fields to ensure needle position is precise up to the sensitivity of the EM probes. The EM system relies on a planar field generator utilizing two coils to create a magnetic field. The stylet probe has a small current running through the length of the stylet, terminating at a position 5mm from the tip of the probe. Through this mechanism, the tracking system bypasses the need for acoustic information of tissue, depending on magnetic flux in EM space to render position and orientation of a sensor device.

In many instances these tracking tools have allowed for sub-millimeter accuracy in the clinical environment [10]. With respect to the guidelines set forth by the AAPM and GEC-ESTRO, requiring sub-millimeter accuracy in needle placement in phantoms, a stereotactic system based on these two modalities would possibly become feasible in the near future [6].

This work sets the stage for the use of EM tracking to mitigate needle trajectory error produced by the speed of sound variance in soft tissue. In order for the feasibility of the system to be evaluated, we assess the accuracy of the EM tracking system and characterize speed of sound within soft tissue phantoms. In this way we hope to establish a baseline procedure and accuracy for taking measurements and using them as inputs for a correctional image-processing algorithm. We will demonstrate the effects of changes in dosimetry due to patient specific SOS variances and the ability to mitigate this aspect dose delivery uncertainty.

Specifically, permanent seed implant brachytherapy utilizes US images for creating plans for treatment. This modality relies on the integrity of the US images to make accurate plans. However, these images do not always represent a precise reflection of distances due to SOS variance. Here we will highlight changes in US images of permanent seed implant plans.

Materials:

Phantoms:

Gelatin phantoms were constructed by varying concentration of powdered porcine gelatin from 6-20% with deionized water (Sigma Aldrich, USA).

EM Tracking:

A local magnetic field was produced with a planar field generator that encompasses a 500mm x 500mm x 500mm cubic space. Sensor probes provided from the manufacturer allow for a 3D coordinate readout from the Aurora Toolbox software interface developed by NDI, capable of tracking up to 8 sensor probes with a 40 Hz frame rate. These coordinates will be compared to the ultrasound output to establish measurement differences. The planar field generator operates at a frequency under IEEE safety standards of 0-3kHz (NDI, Waterloo, Canada).

Template and US calibration:

The template used for SOS estimation and brachytherapy procedures in figure 1 shown below, with 1.8 mm sized and 5mm center-to-center spaced holes. The coordinates of this grid are aligned to the ultrasound monitor to correspond to planned positions for needle or catheter insertion. The grid is placed adjacent to the perineum or phantom and the tracking probe is inserted trough one of the 13 rows and one of the 13 columns.

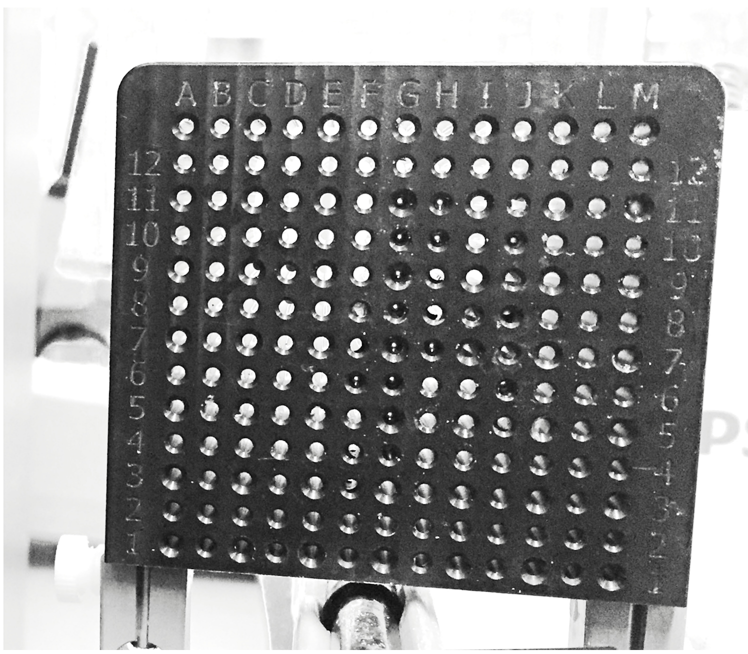

Figure 1. Template grid typically used in brachytherapy procedures. 13 rows are shown, with 13 being unlabeled and 13 columns A through M.

Ultrasound:

Philips (Amsterdam, The Netherlands) PureWave CX50 3D US with Trans esophageal transducer 2D linear array. Using b-mode, 2D images were acquired with a 2 -7 MHz frequency range with a 2500 element X7-2t probe.

Methods:

Phantom Construction

To simulate the varying SOS encountered in soft tissue subtypes, phantoms were constructed with different concentrations of gelatin and other additives. Non iodized NaCl was added to accelerate the speed of sound and olive oil was used to produce the opposite effect. A brass reflector (figure 2) was used to measure differences in time of flight in two cases: one with the sample and another without, thus the SOS was calculated using these cases and equation below.

Speed of Sound Calculation in water tank: $C_S = \frac{1}{\frac{\Delta t}{2D}+\frac{1}{C_w}}$ (1)

C_s = measured speed
C_w= speed in DI water (1482.3 m/s)
Δt = change in reflection time (with sample and without sample)
D = sample thickness

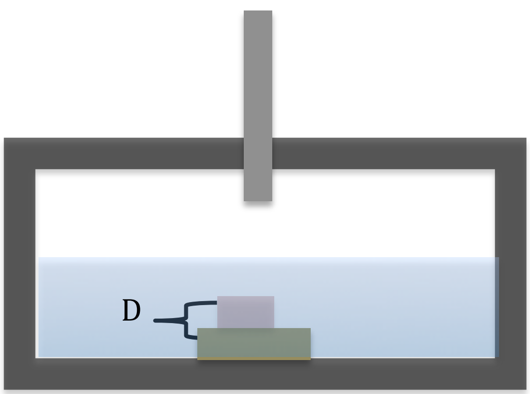

A. Schematic

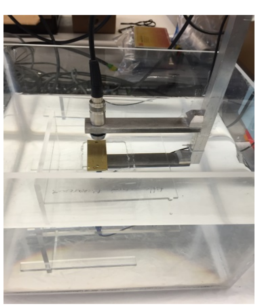

B. Water Tank System in lab

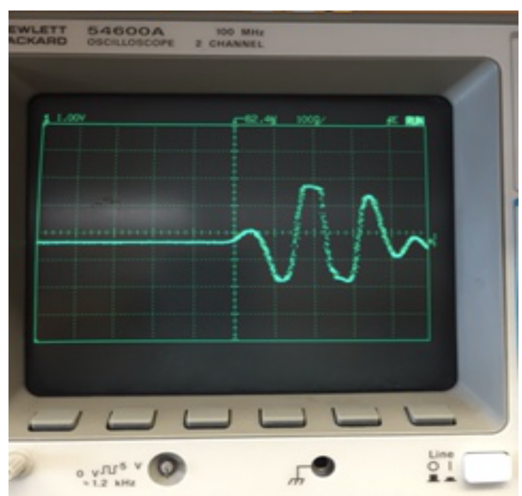

C. Trace recorded on oscilloscope

Figure 2. (A) Represents a schematic of the measurement system and the equation to calculate the speed of sound, a simple brass reflector (B) covered by a sample will

result in echoes with a different time able to be seen and recorded on the oscilloscope (C) .

Table I. Experimental Speed of Sound values: the table below describes the set of experimentally recorded speed of sound values for each medium along with its components.

Medium (sample thickness)	**SOS (m/s)**
Water	1482.7
Gelatin 6 % [m/v] (9mm)	1499.2
Gelatin 8 % [m/v] (9mm)	1505.3
Gelatin 10 % [m/v] (9.5mm)	1506.2
Gelatin 12 % [m/v] (9.52mm)	1530.2
Saltwater Phantom 150g/L salt, 20% gelatin (9.5mm)	1707.1
Saltwater Phantom 150g/L salt, 15% gelatin (9.5mm)	1677.7

Using phantoms with SOS values in the range of soft tissue, the amount of error at different depths can be measured. TRUS images can be analyzed using a caliper tool of the CX50 system to measure depth. This will be compared to the EM coordinate readout to evaluate the difference between the two measurements as well as ground truth. The accuracy of the EM provides a potential gold standard for localization of needles within volumes of interest. The proceeding work will entail assessment of the error, how TRUS image reconstruction contributes to this error at different grid positions and, a method to solve the issues regarding these errors via an image-processing algorithm on b-mode (2D) images.

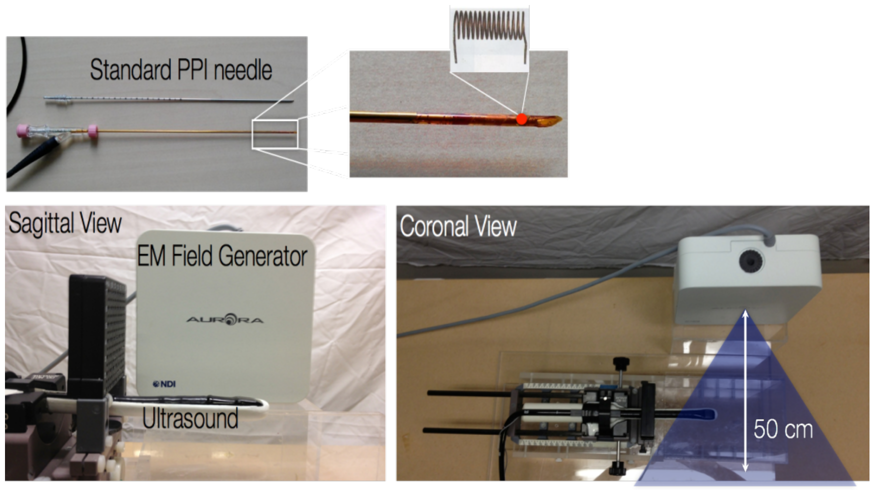

Figure 3. Top left: tracking needle developed by Philips, top right: coil located at terminal end of needle, bottom left: ultrasound probe, template, and field generator, bottom right: system in typical distance from generator.

SOS EM measurement:

Ultrasound images are composed of returning echoes from reflections and scatter, therefore the time variable constitutes the main components of distance and speed measurements.

Equation 2. Time for a reflection to return at a specific depth and velocity.

$$t = \frac{2D}{v}$$

Time of reflection, defined as the distance traveled divided by the speed of sound allows for us to have distance at different speed of sounds, using the same time readout we set these to be equal between 2 different conditions.

Equation 3. Proportion using the same time value to describe different distances measured.

$$\frac{2D_1}{1540} = \frac{2D_2}{SOS}$$

Analyzing the difference in distance readings between a more accurate modality such as EM tracking, which is not perturbed by SOS variance as ultrasound allows us a way to derive the speed of sound in a medium.

Equation 4. SOS measured as a function of difference in depth measurement between EM and Ultrasound

$$SOS = \frac{1540D_2}{D_1}$$

By using the preceding equations, a speed of sound more representative of a sample's acoustic properties is able to be approximated.

Figure 4: Brachytherapy system, including stylet, ultrasound probe, and field generator in laboratory environment. EM probes are located underneath the transducer head, 5 mm from the distal end of the stylet, and below the template grid.

EM Accuracy:

The Accuracy of the planar field generator (figure 3) has been previously characterized in Bharat et al, and these characteristics were confirmed using the template of the brachytherapy system in the lab (figure 4) [11]. The template grid spacing has 5 mm between each adjacent position with 13 rows and 13 columns, which was measured using calipers. The difference between the physical measurement and EM measurement is shown in the table below for 60 of these positions. The EM has an average difference of 0.5 mm, an RMS of 0.55 mm and SD of 0.24 mm, adhering to the manufacturer's calculations of uncertainty in 0.48-0.78mm for a given sensor.

Table II. Physical distance measurement minus EM distance measurement: 60 different position of the template grid were used to assess the EM accuracy. The difference in distance recorded by EM and ground truth are shown below.

Grid position	A (mm)	D (mm)	G (mm)	J (mm)	M (mm)
13	0.65	0.74	0.61	0.71	0.89
12	0.62	0.75	0.48	0.78	0.85
11	0.60	0.75	0.49	0.66	0.82
10	0.54	0.64	0.39	0.60	0.73
9	0.55	0.58	0.33	0.58	0.85
8	0.47	0.50	0.23	0.49	0.71
7	0.44	0.47	0.22	0.36	0.69
6	0.36	0.44	0.10	0.31	0.76
5	0.40	0.38	0.11	0.27	0.67
4	0.50	0.38	0.0	0.22	0.62
3	0.38	0.38	-0.08	0.18	0.71
2	0.36	0.44	-0.07	0.22	0.78

Table III. EM Accuracy Summary: mean difference values or the average of the difference between the ground truth measurements recorded by caliper and the EM measurements along with the standard deviation, and rms are noted below.

Mean difference (mm)	0.50
RMS (mm)	0.55
SD (mm)	0.23

Image Correction:

Using Equation 4 mentioned above, we are able to achieve an input for an image correction algorithm. Image reconstruction in a phased array system utilizes one element as the center or origin of image formation. All distances in the field of view are measured as the distance from this point and the position of the returning echo. These echoes are encoded as a function of time in the ultrasound electronics with corresponding pixel intensities indexed as a function of the returning echo time and angle.

In order to correct for instances in which the SOS of the tissue is above the SOS of the calibrated US value, spline grids may be used to map pixels to a more precise location. The vector maps below figure (5) indicate the model of image correction. In the axial direction error propagates linearly from the transducer face, this effect is similar in the lateral direction, but originates from the central element of the transducer. Thus the corresponding shift is modeled as a gradient, with increasing shifts in the peripheral zones of the image. The gradient consists of the distance that should be seen if calibrated to the correct SOS.

Axial Vector Map describing pixel shift

Lateral Vector Map describing pixel shift

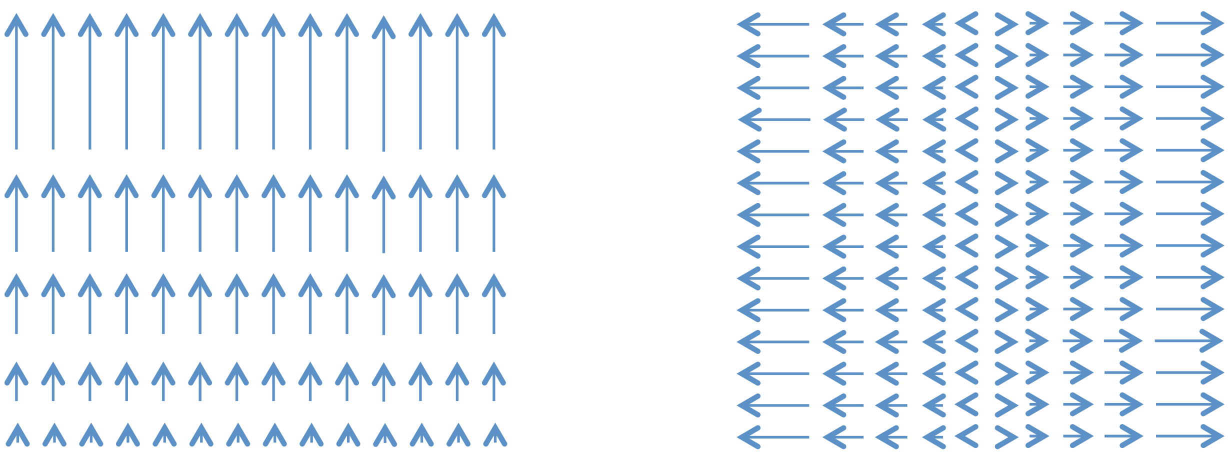

Figure 5. These spline grids or vector maps describe the movement of pixels away from the transducer element. This situation represents the case which a prostate has a higher speed of sound than 1540 m/s. The error propagates as a function of distance with the vectors increasing in magnitude as they increase in distance from the origin of the transducer.

<u>Meta data manipulation:</u>

Alternatively, since the propagation of error occurs in steps between adjacent pixels, the header information stored on a DICOM image can be manipulated to take this into account. Resolution of the pixels themselves can be changed to account for the speed of sound error. The input for this method requires calculation of a scaling factor, defined as SOS/1540 to be multiplied by the pixel dimensions in x and y stored as “physical delta x” and “physical delta y” in the metadata. However, this method cannot easily handle complex situations for the future in which zones of tissue contain different acoustic velocities.

Orientation of the System:

The method of approximating SOS using EM relies on the assumption that the origin is located at the center of the transducer face. This origin of the imaging element can be easily placed if the transducer is aligned with the central column of the template grid, however this may not be the case in clinical context, in which the probe must be oriented to have optimal imaging for patient-specific anatomical reference. Taking this into account, the planar field generator is able to read out quaternion coordinates: these coordinates describe a vector generated by the field generator in 3D coordinates, as well as the angle about this vector.

This information is useful in corroborating the amount of roll, pitch and yaw that occurs to the origin in order for proper placement of the imaging element in EM coordinate space. Orientation becomes an important determinant when analyzing the distance between two modalities, as the origin must be centered in common space to have a direct comparison of the two different methods. Taking into consideration the angulation of the transducer, quaternion values produced by the EM system are able to provide information for calibrating the origin. The quaternion values q0, qx, qy, and qz output by the EM system can be used to achieve a rotation matrix describing the amount of angle about a vector. Knowing the 3D coordinates of the sensor probe located dorsal to the transducer face, a reference point can be established to recognize the amount of roll pitch and yaw about the transducer.

Using the quaternion and vector coordinates, the vector can be transformed into the probe coordinate space, applying any translations to define the center element of the transducer and then applying the inverse quaternion transformation to replace the coordinate with respect to EM coordinates.

Results:

SOS Estimation

The table containing trials 1-3 below indicate three different trials in which gelatin phantoms were tested to approximate the SOS using the ratio of EM to US distance. Once a coordinate was recorded when the sensor coil of the stylet entered the imaging plane, this was the compared to the ultrasound distance within a particular phantom. The ratio of the EM distance to the ultrasound distance was then multiplied by 1540 m/s to achieve the estimated SOS. Overall the results indicate that we are able to calculate the speed of sound within these phantoms to 1% accuracy. The columns and rows describe the corresponding columns and rows on the template grids, which are labeled A-M and 13-1 respectively.

Table IV: SOS estimation, using different gelatin samples

Trial 1 (Measured SOS in water tank = 1677.8) Percent Error (%)			
Row number	Column A	Column G	Column M
13	0.13	0.4	0.15
11	0.06	0.13	0.24
9	0.06	0.15	0.35
7	0.54	0.46	0.034
5	0.65	0.08	0.59
Calculated SOS using ratio of EM to US (m/s)			
Row Number	Column A	Column G	Column M
13	1680.1	1684.6	1675.2
11	1676.7	1675.6	1681.9

9	1678.8	1675.1	1683.8
7	1668.7	1669.9	1678.4
5	1688.7	1676.3	1687.8

Trial 2 (**Measured SOS in water tank = 1698.1) Percent Error (%)**					
Row Number	Column A	Column D	Column G	Column K	Column M
13	0.12		0.44		0.25
10		0.07		0.16	
9	0.34		0.2		0.15
7		0.25		0.29	
6	0.9		0.19		0.73
Calculated SOS using ratio of EM to US SOS (m/s)					
Row Number	Column A	Column D	Column G	Column K	Column M
13	1696		1690.5		1693.8
10		1699.4		1700.9	
9	1704		1694.6		1700.7
7		1702.5		1703.1	
6	1713.5		1701.3		1710.6

Trial 3 (**Measured SOS in water tank = (1535.5 m/s) Percent Error (%)**)			
Row Number	Column A	Column G	Column M
13	0.93	0.01	0.24
11	0.65	0.2	0.13
9	0.91		0.22
7	1.88	1.03	0.86

Calculated SOS using ratio of EM to US SOS (m/s)			
Row Number	Column A	Column G	Column M
13	1549.8	1535.3	1539.2
11	1545.6	1538.6	1537.5
9	1549.6		1539
7	1564.4	1551.4	1548.8

Mean Percent Error	0.40
SD Percent Error	0.37

Uncertainties

With the three major components of our system, the uncertainties are outlined as such: error of the EM system, error of the image correction process, and the speed of sound water tank measurements. The EM system shows to have a mean error of 0.5 mm and SD of 0.23 mm from ground truth measurements when placed in a lab environment. Experimental values show that the mean percent error is calculated to be 0.4% over 39 trials when using the SOS estimation.

The image correction process has an error of 0.96% percent which is possibly due to the rounding that occurs when a pixel is shifted halfway between two rows or two columns and must choose to round up to the next row or column. This can be corrected if a 0.5 mm offset is subtracted from the corrected measurements or otherwise add an interpolator to take this into account. However, an interpolator may not show the most precise anatomy, as it averages or uses another method to fill the intensity values between pixels. Using the 0.5mm offset, the algorithm performs the image correction with an average error of 0.27%. Great care must be taken when drawing the measurement ROIs.

Adding these error values, the mean error of using the system for SOS estimation and image correction should to be around 1% (or .8-1 mm). Taking into consideration that 2-4 mm errors occur during conventional seed implant brachytherapy procedures, our system is a viable way of mitigating this error, realizing approximately sub-millimeter accuracy.

<u>Dose Distribution:</u>

The following images depict changes in dosimetric plans due to these image corrections. On the left represents a plan for a patient's prostate accordingly planned on the uncorrected image. On the right represents a plan with the corrected image for a prostate plan based on a SOS of a higher value 1613 m/s.

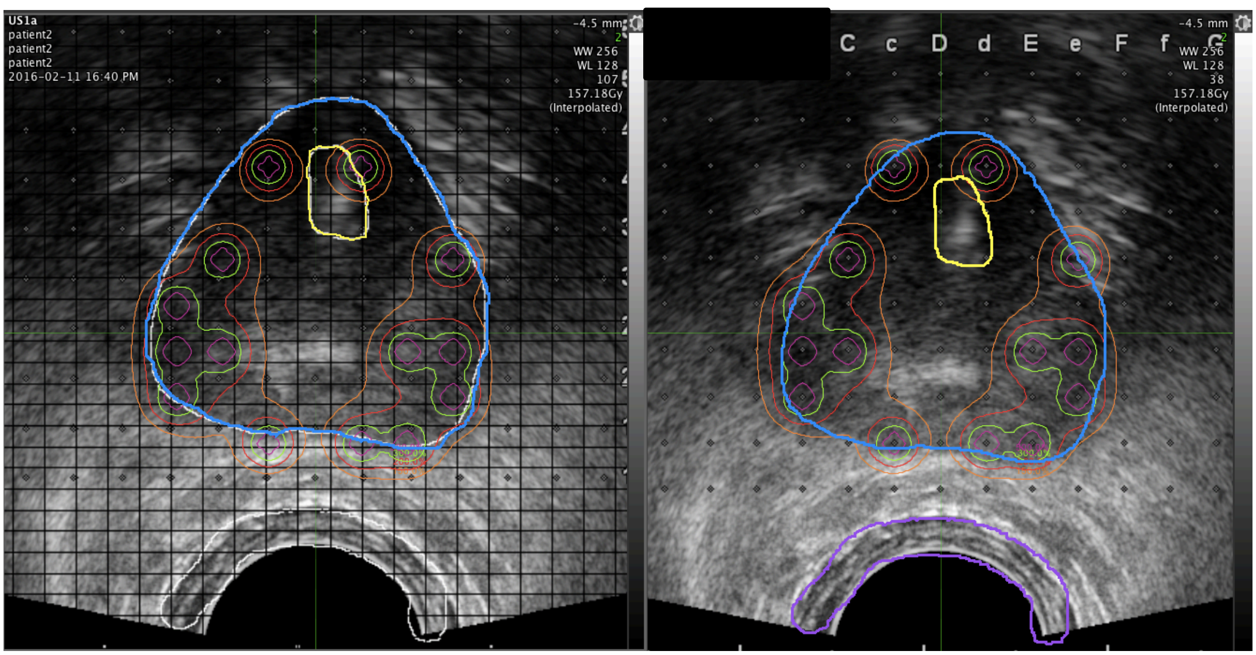

Figure 6. A typical dosimetric plan based on ultrasound imaging using a treatment planning software. The uncorrected plan is located on the right and a corrected plan with a speed of sound based on 1613 m/s is located on the left. The prostate and urethra are both contoured in blue and yellow respectively on both images, with the rectum as purple on the right and white on the left. The remaining contours represent isodose curves: orange curve represents the 150%, red is 200%, green 300% and magenta as 500%.

Patient 1

In this uncorrected image (figure 6 right side) the ultrasound planning involves the placement of a seed nearby the anterior right most portion of the prostate. This is in close proximity with the urethra contour in yellow. If the true speed of this prostate was 1613 m/s, the corrected image on the left shows the orange 150% isodose curve to show aggressive overlap into the urethra. In addition the amount of dose not treating the regions towards the posterior end of the prostate must also be noted. The seed may also rupture or be completely implanted in the urethra in this hypothetical procedure. Furthermore, the 300% isodose curve in green and 500% isodose curve in magenta show intrusion into the urethral contour as well.

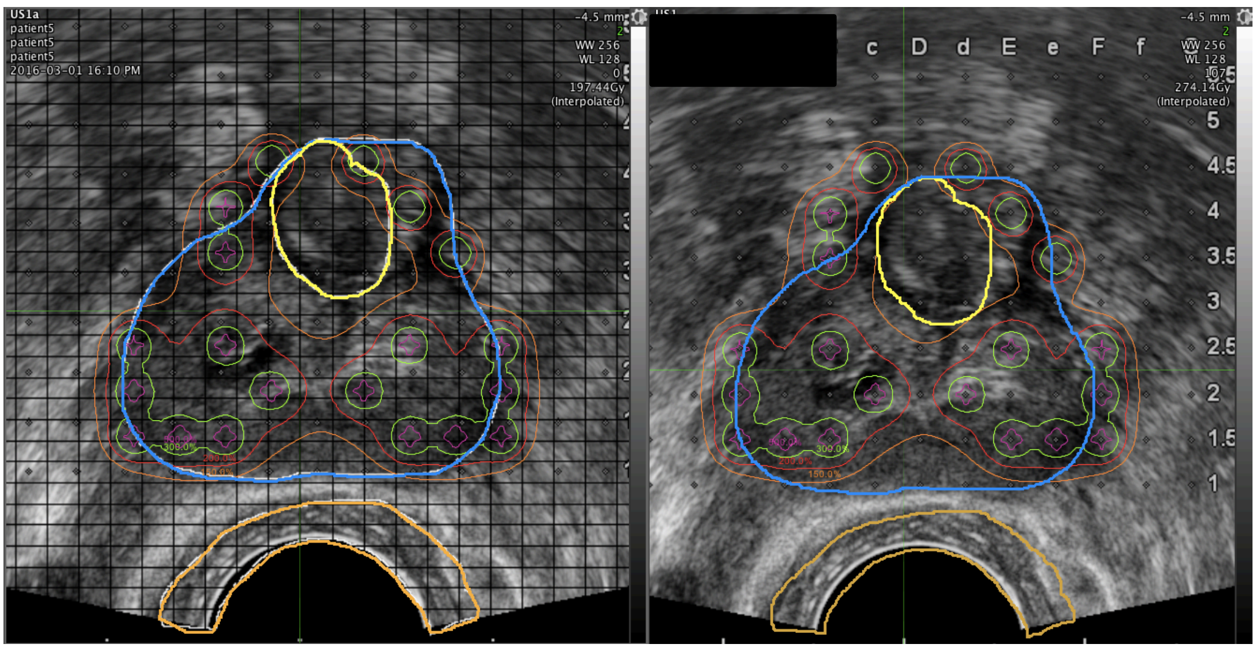

Figure 7. Another dosimetric plan based on ultrasound imaging using a treatment planning software. The uncorrected plan is located on the right and a corrected plan with a speed of sound based on 1613 m/s is located on the left. The prostate, urethra, and rectum are contoured in blue, yellow, and gold respectively on both images. The remaining contours represent isodose curves: orange curve represents the 150%, red is 200%, green 300% and magenta as 500%. In this case the urethra appears to be free of significant overlap, however the corrected image shows intrusion of the 150%,200%, and 300% isodose curves into the urethra.

Patient 2

Many of the same effects as the previous patient can be seen, this time with two seeds showing overlap into the contour of the urethra in the corrected image (figure 7). The urethra in this patient appears more anteriorly located on the prostate with larger contours. This enables the opportunity for dose to enter into the urethral contours; one of the main causes of urinary morbidity.

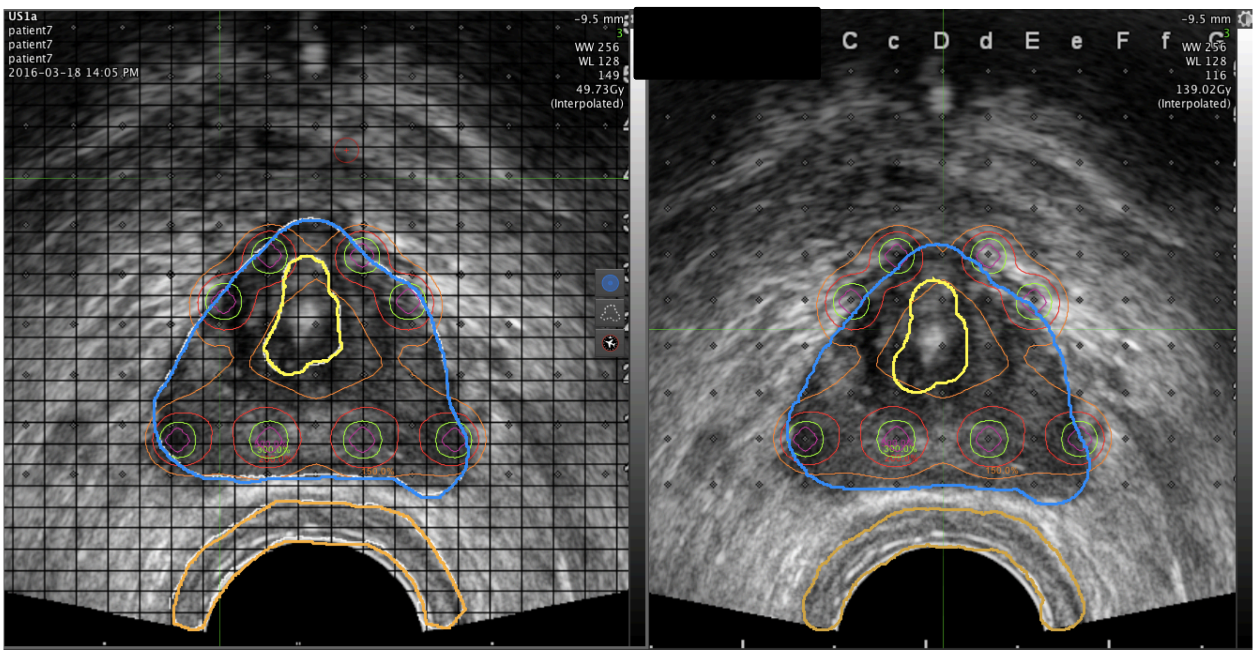

Figure 8. This dosimetric plan has the same contouring scheme as figure 6, with the corrected image on the left based on 1613 m/s and the uncorrected based on conventional speed of sound calibrated in the clinic. The 200% isodose curve intersects with the urethra and there is more of an apparent overlap with the orange 150% isodose curve.

Patient 3 This image (figure 8) is similar to figure 5 with the 2 seeds greatly affecting the amount of overlap of the 150% isodose contours with the urethral contours in the corrected image on the left. In addition, the seeds most anterior to the prostate are located within the contours of the prostate, which is not seen on the uncorrected plan. If this occurs in multiple slices of the acquisition, significant differences in dosimetry occur.

Discussion:

The significance of this work primarily revolves around the organ at risk sparing techniques and allowing for proper amount of dose to be represented by a planning technique. The urethra is known to be a continuous organ, which can be affected in function if agitated or maligned in any place along the length of the organ. Thus differences in dose may not be so apparent in the planning software, but the compelling images showing the isodose curves directly overlapping the primary organ at risk demonstrate the capability of our process to minimize these issues.

The developed technique is versatile and applicable to other brachytherapy procedures outside of the prostate. The amount of SOS variance in breast, liver and kidney is also appreciable and would lend themselves to a correction approach as outlined herein. [11].

Other methods involving SOS correction measures in-vivo may involve the use of ionizing radiation to approximate this characteristic [12]. In contrast, we have demonstrated a way to approximate the SOS with close to 1% accuracy with ultrasound in conjunction with EM, without additional dose. In the event which many needles and catheters must be placed for a brachytherapy procedure, non-ferromagnetic components must be utilized in order to avoid compromising the accuracy of the EM system. Error values of the system can be surveillance real time to ensure fewer inaccuracies during the treatment. In a clinical setting with LCDs, surgical tools and needles,

Another caveat of our system is the intersection of the stylet sensor and imaging plane of the ultrasound. In the occurrence that the EM coordinate produced by the sensor is out of plane with respect to the imaging device, any bending or angulation of the stylet will produce a coordinate unrepresentative of the site being imaged resulting in error of SOS approximation. This can be solved if a 6 degree of freedom (DOF) sensor is utilized, and we can achieve the orientation of the entire tool to designate the point of intersection between the imaging plane and the sensor to locate the adjusted coordinates of the probe.

A limitation to this simulation is that it assumes uniform SOS within the tissue. Heterogeneous tissue where the SOS varies significantly would cause an averaging of the zone in the field of view. This problem is outside the scope of our trials, as we constrain our problem to tissue as a 1-component analysis.

With the new age of advanced robotics, automatic procedures may allow for better accuracy and health outcomes with difficulties in communication between treatment planning and robotic systems being overcome; Cunha et al have enabled the use of a complex device capable of 'seamless' clinical workflow in ex vivo MR brachytherapy procedures [14]. However, this technique relies on prior imaging and planning to correspond correctly. With the advancement of ultrasound technology to take into account the SOS variances, real time image calibration may be carried out on the fly, allowing for real time plan adjustments.

Other research has indicated the development of ultrasound robotics to accurately place the needle with sub millimeter accuracy, however these systems cannot account for large differences in SOS from the calibrated value [15]. Stereotactic surgery relies on the fact that the coordinate system is accurately represented when overlaid on the anatomy. However, in instances that the organ has a different SOS than calibrated, issues occur regarding the representation of distance and consequently the coordinates recognized by the robotics. Our technique developed through EM tracking in combination with ultrasound imaging may provide a practical solution for taking into account SOS variances. This could also provide a consistently accurate robotic system that may be used in complex areas of tissue with multiple SOS's for the future.

Conclusion:

The utilization of EM based spatial corrections to mitigate systematic SOS uncertainty in US images permits more precise cancer therapy by improving the spatial fidelity of radiation sources in stereotactic systems We have demonstrated the ability to approximate the speed of sound within a sample using custom-fabricated phantoms to within 1% of measured values in a controlled water tank setting. With the power to account for differences in speed of sound, planning software will take advantage of corrected images to provide more accurate conformal therapy. Ultrasound based brachytherapy will be also be able to move away from the issue of manual seed implantation, resulting in potentially faster procedures, less human error, and improved health outcomes. Translating this to practice in vivo renders itself as the next target regarding the development of precision stereotactic robotics.

The current state of stereotactic brachytherapy using ultrasound image guidance does not include a way to compensate for SOS variance. Using EM tracking, other organs considered for brachytherapy treatment using ultrasound image guidance may also be corrected for variance in speed of sound. This includes breast, kidney, liver amongst other organs imaged by ultrasound during radiotherapy.

References

1. Feldman MK, Katyal S, and Blackwood MS. US Artifacts. RadioGraphics 2009 29:4, 1179-1189. doi:10.1148/rg.294085199

2. Fontanarosa D, Meer S, Gurp Esther B, Stroian G, and Verhaegen F. Magnitude of speed of sound aberration corrections for ultrasound image guided radiotherapy for prostate and other anatomical sites. Medical Physics 39, 5286 (2012); doi: 10.1118/1.4737571

3. Ng A and Swanevelder J. Resolution in Ultrasound. Contin Educ Anaesth Crit Care Pain(2011) 11 (5): 186-192.doi: 10.1093/bjaceaccp/mkr030

4. Hoheisel M. Needle and catheter navigation using electromagnetic tracking for computer-assisted C-arm CT interventions. Proceedings of SPIE – The international society for optical engineering. March 2007.

5. Curry TS, Dowdey JE, Murry RE. Christensen´s physics of diagnostic radiology 4 Ed. Lippincott Williams & Wilkins. (1990) ISBN:0812113101.

6. Poder TK et al. AAPM and GEC-ESTRO guidelines for image-guided robotic brachytherapy: Report of Task Group 192. Medical Physics. 2014. doi:10.1118/1.4895013.

7. Tudor D and Zhang D. A novel method for accurate needle-tip identification in trans-rectal ultrasound-based high-dose-rate prostate brachytherapy. Brachytherapy. December 2011.

8. Surveillance, Epidemiology, and End Results (SEER) 18 registries, National Cancer Institute, 2015.

9. K. Elliott, K. Wallner, G. Merrick, et al. Medical malpractice of prostate brachytherapy Brachytherapy, 3 (2004), pp. 231–236.

10. Yaniv Z, Wilson E, Lindisch D, Cleary K. Electromagnetic tracking in the clinical environment. *Medical Physics*. 2009;36(3):876-892. doi:10.1118/1.3075829.

11. Bharat S, Kung C, Dehghan E, et al. Electromagnetic tracking for catheter reconstruction in ultrasound-guided high-dose-rate brachytherapy of the prostate. Brachytherapy. 2014;13:640–650.

12. Wood et al. Electromagnetic Tracking for Thermal Ablation and Biopsy Guidance: Clinical Evaluation of Spatial Accuracy. Journal of Vascular Interventional Radiology. September 2007.

13. Duck FA. Physical Properties of Tissue. Academic Press. London. 1990.

14. Cunha, J. A. *et al*. Toward adaptive stereotactic robotic brachytherapy for prostate cancer: demonstration of an adaptive workflow incorporating inverse planning and an MR stealth robot. *Minim. Invasive Ther. Allied Technol.* **19**, 189–202 (2011).

15. Fichtinger, G. et al. Robotic assistance for ultrasound-guided prostate brachytherapy. Med. Image Anal. 12, 535–545 (2008).

Publishing Agreement

It is the policy of the University to encourage the distribution of all theses, dissertations, and manuscripts. Copies of all UCSF theses, dissertations, and manuscripts will be routed to the library via the Graduate Division. The library will make all theses, dissertations, and manuscripts accessible to the public and will preserve these to the best of their abilities, in perpetuity.

Please sign the following statement:

I hereby grant permission to the Graduate Division of the University of California, San Francisco to release copies of my thesis, dissertation, or manuscript to the Campus Library to provide access and preservation, in whole or in part, in perpetuity.

Author Signature

09/05/2016

Date